

A Switching Event-Triggered Model Predictive Control for HVAC Systems

Mojtaba Sharifzadeh¹^a, Hani Beirami¹, Federico Bonafini², Matteo Campidelli², Roberto Cavada¹,
Alessandro Cimatti¹^b and Stefano Tonetta¹^c

¹Fondazione Bruno Kessler, 38123, Trento, Italy

²Innova Engineering S.r.l. 38079, Tione di Trento, Italy
{ssharifzadeh, hbeirami, cavada, cimatti, tonettas}@fbk.eu,
fi

Keywords: Event-Triggered MPC, HVAC, Modeling, System Identification, Switching Control.

Abstract: Heating, ventilation, and air conditioning (HVAC) systems have great potential for energy savings and integration with green energy sources. Advanced control of these systems could play a key role in optimizing consumption while enhancing efficiency and performance. In this paper, a new model-based methodology is proposed for real-time control of the compressor in HVAC systems, based on switching event-triggered model predictive control. The approach manages the switch among different operational modes and provides the possibility to set different constraints to be optimized, enabling a multivariable scheme. It also applies the latest model-based design standards derived from the AUTOSAR framework to adapt them for an HVAC platform that offers substantial technical value, while also preserving the model-based design structure for improved lifecycle management. The models used for the controller in each modality are developed through the system identification standards and validated using data acquired from the air-water heat pumps in the test field. The effectiveness and performance of the control approach are also demonstrated through Model-in-the-Loop (MIL) testing.

1 INTRODUCTION

In recent years, especially since carbon emissions have become a serious global issue, substantial research has focused on enhancing the control of heating, ventilation, and air conditioning (HVAC) systems. Given that buildings constitute a significant proportion of global energy consumption, improving the energy efficiency of building structures is crucial for reducing energy consumption on a global scale. The traditionally used controllers in buildings often rely on feedforward mechanisms or traditional control strategies, which may not be the most efficient for energy management (Soyguder et al., 2009).


Several studies on HVAC systems focused on designing various control strategies to enhance system management and efficiency using PID-based classical approaches due to their practical feasibility. However, these strategies often suffer from a lack of real-time


tuning for the controller, as they are not sufficiently robust, and encounters problems when dealing with multivariable models (Soyguder et al., 2009; Blasco et al., 2012).


In recent works (see, e.g., (Taheri et al., 2024a)), Model Predictive Control (MPC) has emerged as a standout approach due to its ability to manage multiple variables and provide optimized outcomes within a set of constraints which makes it a great potential for use in intelligent buildings, enhancing control, and achieving greater energy savings.

MPC employs a dynamical model to predict the anticipated dynamics of the system over a specific timeframe. These predictions are then used to formulate an optimization problem designed to minimize a defined cost function, which usually measures system performance.

MPC represents a flexible technique, particularly effective for multi-input, multi-output (MIMO) control challenges characterized by notable interactions between the inputs being manipulated and the outputs being controlled. A primary benefit of MPC, compared to other model-based control strategies, is its

^a <https://orcid.org/0000-0002-0552-1951>

^b <https://orcid.org/0000-0002-1315-6990>

^c <https://orcid.org/0000-0001-9091-7899>

capability to easily incorporate inequality constraints on variables, including both upper and lower bounds on inputs or outputs (Darby and Nikolaou, 2012).

There is a considerable volume of literature regarding the application of MPC to HVAC systems (Taheri et al., 2024a; Saletti et al., 2020; Yao and Shekhar, 2021a). However, none of previous works yet offered a comprehensive platform in this context, capable of dealing with the different operational modes typical of HVAC systems (e.g., heating, cooling, and defrost).

In this paper, we aim to develop a switching event-triggered model predictive control for HVAC systems, which reacts to external events to switch between different modalities. We implement and evaluate the approach on an industrial real system, which uses legacy control software. We begin by processing the data acquired from HVAC machines during field tests, which involves standardizing formats, applying filtering methods, resampling, and performing data interpolation. We then develop a model of the dynamical behaviour used to design a multi-variable controller. We use standard system identification techniques to create a model from the data in different modalities. We then design the switching MPC, thus an MPC for different modalities and a switch logic with a state machine that activates the various controllers. Finally, we focus on validating the effectiveness of the model as well as switching MPC methodology. This step includes both the validation of the identified models in the different modalities as well as the evaluation of the system's switching behaviour under simulated conditions.

The organization of the current manuscript is as follows. In section 2, the related works are given. In section 3.1 the problem is described in more detail. In the next sections, the model, data acquisition and system identification and successively the switching control approach implementation, are presented respectively. The results are given in section 6, and eventually, conclusive remarks are presented in the last section.

2 RELATED WORKS

In (Afroz et al., 2018), various modeling techniques used in HVAC systems are studied, assessing their applicability, strengths, and weaknesses, together with their impact on energy efficiency and indoor environmental quality. The existing gaps are highlighted, and various recommendations to enhance the performance of building HVAC systems are given. In (Taheri et al., 2024b), it is demonstrated through simulation that the

Model Predictive Control (MPC) approach provides a 7% greater reduction in energy consumption compared to the classical PID method when applied to HVAC systems in commercial buildings. In (Staino et al., 2016), two different optimization scenarios (selfish and cooperative) are focused on the analysis of the performance of MPC in the heat pumps of buildings.

Saletti et al. proposed a novel control methodology using MPC for district heating networks, aimed at optimizing thermal energy distribution to buildings using a new optimization algorithm (Saletti et al., 2020). It is demonstrated that it gives significant reductions in energy consumption and improved indoor comfort, compared to conventional controllers. However, it is based on a linearized approximated model that does not always reflect the real characteristics of the system.

In (Yao and Shekhar, 2021b), a comprehensive analysis has been conducted in terms of implementation, optimization, application, and modeling, as well as the overall scheme in the context of MPC for HVAC systems. However, the need for a more realistic model that predicts the outlet thermal water dynamics has not yet been met. Additional work is required to achieve optimized output control and to provide an improved dynamical behavior for the MPC controller. Specifically, for HVAC systems, the need to switch in real-time between MPC controllers has received only limited attention in the literature. It is concluded that the application of MPC in the HVAC field remains a wide-open subject, with much work still to be done.

3 SYSTEM DESCRIPTION

In this section, we give a high-level description of the problem context and the specific use case under consideration. In the following sub-section, we focus on the system characterization.

3.1 Problem Description

Our objective is to re-design with a model-based approach the control of real industrial heat pumps that are already in operation and that we can test to collect data. In particular, The tested heat pump units come in a range of power capacity sizes to suit different needs, ranging from 5 kW to 15 kW nominal capacities. These units offer various installation options to accommodate different space and aesthetic requirements. The installation options include traditional setups, vertical and horizontal outlet configu-

rations, concealed installations, and more. Furthermore, the heat pump units can be configured with or without Domestic Hot Water (DHW) systems and support both heating and cooling applications within the plant setup. For space heating and cooling, the units can be paired with fan coil units, radiant systems, or a combination of both, providing flexibility to meet specific climate control needs. This versatility ensures that the heat pump units can be tailored to fit a wide range of residential or commercial applications. This justifies even more the need of an advanced control system that can be adjusted, fine tuned and finally verified with model based techniques and tools.

The control system operates in seven distinct modalities: Heating Plant, Heating DHW, Cooling Plant, Defrost Mode, Off by User Intervention, Off by Alarm, and Off by Thermal Condition. Depending on the conditions, it must switch between these modalities in real-time. The Defrost Mode is a crucial operational phase designed to remove accumulated ice on the Air Exchanger during the Heating Plant under cold weather conditions. Off by User Intervention is a modality in which the heat pump/compressor goes off due to user intervention. If there is an alarm, according to predefined logic, the machine or compressor deactivates, and this state is referred to as Off by Alarm. When all the target temperatures are achieved, the compressor turns off within the modality of Off by Thermal Condition. The desired temperature is defined by the water target temperature at the outlet of the water exchanger.

The model used for the controller is expected to be obtained and validated with acquired data from one of our heat pump machines in the testing field (see Fig. 1). The data from these heat pumps, equipped with different sensors, is collected through Modbus communication interfaces and transmitted to custom dataloggers based on embedded Linux systems, which send the data securely to a central server in the cloud for storage in InfluxDB and visualization by Grafana.

3.2 System Characterization

In the context of the HVAC system, thermodynamics could be applied to their various components to describe how energy behaves within such systems, which typically take the form of partial differential equations (PDEs). It generally involves the terms representing different energy transfer mechanisms. It is important to recognize the inherent complexity and nonlinearity of the derived PDEs that describe the energy balance in HVAC compressor systems. These equations capture the detailed physical processes and interactions within the system, making them difficult



Figure 1: The water-air heat pump under test in the experimental field.

to model and understand, especially for real-time control applications. The nonlinearity in these equations arises from the interconnection of various factors including the nonlinear behavior of heat transfer and fluid flow phenomena within the system.

Below, we give a dynamical representation of the model to introduce the critical variables of the control system. The simplified nonlinear overall state-space structure, derived from the dynamic energy balance equation of the HVAC system, serves as a gray-box equivalent for thermodynamically derived equations. It also provides a dynamic representation of the physical model at the microscale level where could be given as Equation 1:

$$\begin{cases} \dot{x}(t) = f \left(x(t), \begin{bmatrix} Comp_{Freq}(t) \\ S_{EEV}(t) \end{bmatrix}, \begin{bmatrix} WT_{WExIn}(t) \\ RT_{CompDis}(t) \\ T_{air}(t) \end{bmatrix}, v(t) \right) \\ \begin{bmatrix} WT_{WExOut}(t) \\ RT_{WEx}(t) \end{bmatrix} = g \left(x(t), \begin{bmatrix} Comp_{Freq}(t) \\ S_{EEV}(t) \end{bmatrix}, \begin{bmatrix} WT_{WExIn}(t) \\ RT_{CompDis}(t) \\ T_{air}(t) \end{bmatrix}, v(t) \right) \end{cases} \quad (1)$$

which is presented in a standard nonlinear continuous time-invariant state-space form, which includes vectors of state variables $x(t)$, control inputs $u(t)$ shown as $Comp_{Freq}(t)$ and $S_{EEV}(t)$, measured disturbances $w(t)$, and unmeasured disturbances $v(t)$, respectively, repeated for both the nonlinear functions f and g . $Comp_{Freq}(t)$ denotes the compressor speed, $S_{EEV}(t)$ is the Electronic Expansion Valve (EEV) step, $WT_{WExIn}(t)$ and $WT_{WExOut}(t)$ stand for the water temperature at the water exchanger inlet and outlet respectively, $RT_{CompDis}(t)$ is the refrigerant temperature at the compressor discharge, and $T_{air}(t)$ stands for the ambient air temperature. The component control

scheme is presented in Fig. 2, which includes both heating (DHW/plant) and cooling behaviors on the I and II cases, respectively. The Water Exchanger acts as a condenser in the first case and as an evaporator in the second one, while the Air Exchangers act oppositely. The refrigerant flow direction for the Heating DHW and Heating Plant modes is as indicated in case I of Fig. 2. However, the flow direction is reversed for the Cooling and Defrost modes, as illustrated in case II.

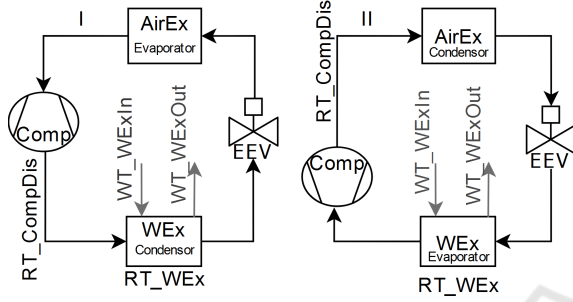


Figure 2: Component Mechanical Scheme.

4 DATA-DRIVEN IDENTIFICATION MODEL

To process the functional model, we start from data acquisition and refinement. This stage forms the essential foundation for optimally preparing the acquired experimental data from our split air-water 11 kW heat pump with R32 refrigerant and facilitating subsequent steps. As said earlier, the data is collected through Modbus communication interfaces and transmitted to several custom dataloggers, which send the data securely to a central server in the cloud for storage in InfluxDB and visualization by Grafana. Data preparation involved standardizing formatting, algorithmic filtering, frequency-based filtering, resampling, and data imputation techniques such as interpolation, forward filling, and backward filling. A significant step following the data preparation phase is to focus on identifying an appropriate model through the System Identification approach. Considering the requirement for a model within the predictive controller to operate efficiently during iterative processes, and given the planned implementation in an embedded system, we selected a structure that is both highly effective and simple for this application.

$$\begin{aligned}
 \begin{bmatrix} x_1(t+1) \\ x_2(t+1) \\ \vdots \\ x_{n-1}(t+1) \\ x_n(t+1) \end{bmatrix} &= \begin{bmatrix} A_{11} & A_{12} & \cdots & A_{1n-1} & A_{1n} \\ A_{21} & A_{22} & \cdots & A_{2n-1} & A_{2n} \\ \vdots & \vdots & \ddots & \vdots & \vdots \\ A_{n-11} & A_{n-12} & \cdots & A_{n-1n-1} & A_{n-1n} \\ A_{n1} & A_{n2} & \cdots & A_{nn-1} & A_{nn} \end{bmatrix} \\
 &+ \begin{bmatrix} x_1(t) \\ x_2(t) \\ \vdots \\ x_{n-1}(t) \\ x_n(t) \end{bmatrix} + \begin{bmatrix} B_{11} \\ B_{21} \\ \vdots \\ B_{n-11} \\ B_{n1} \end{bmatrix} \text{Comp}_{\text{Freq}}(t) \\
 &+ \begin{bmatrix} F_{11} & F_{1n-1} \\ F_{21} & F_{2n-1} \\ \vdots & \vdots \\ F_{n1} & F_{nn-1} \end{bmatrix} \begin{bmatrix} WT_{\text{WExIn}}(t) \\ T_{\text{air}}(t) \end{bmatrix} \\
 WT_{\text{WExOut}}(t) &= \begin{bmatrix} C_{11} & C_{12} & \cdots & C_{1n} \\ \vdots & \vdots & \ddots & \vdots \\ C_{n1} & C_{n2} & \cdots & C_{nn} \end{bmatrix} \begin{bmatrix} x_1(t) \\ x_2(t) \\ \vdots \\ x_{n-1}(t) \\ x_n(t) \end{bmatrix} \\
 &+ D_{11} \text{Comp}_{\text{Freq}}(t) + \begin{bmatrix} E_{12} & E_{13} \\ \vdots & \vdots \\ E_{n2} & E_{n3} \end{bmatrix} \begin{bmatrix} WT_{\text{WExIn}}(t) \\ T_{\text{air}}(t) \end{bmatrix} \quad (2)
 \end{aligned}$$

The chosen model is discretized and linearized to enhance computational efficiency. Additionally, the temperature of the refrigerant is omitted from the model due to its highly nonlinear characteristics, which could complicate real-time computations. The details of the model are presented in Equation 2.

Defining θ as the collection of state-space matrices gives $\theta = \{A; B; F; C; D; E\}$, where A, B, F, C, D and E are the system matrices. Hence, the identification problem is defined as

$$\hat{\theta} = \arg \min_{\theta} \frac{1}{\Psi} \sum_{k=1}^{\Psi} (\epsilon(t_{\text{samp}}, \theta))^2 \quad (3)$$

The prediction error, denoted as $\epsilon(t_{\text{samp}}, \theta)$, is defined as the difference between the actual output $y(t_{\text{samp}})$ and the simulated output of the state-space model $\hat{y}(t_{\text{samp}}, \theta)$ at the sample time t_{samp} given as Equation 4. While Ψ represents the total number of data samples. In this work, Prediction Error Method (PEM) (Ljung, 1998) is addressed through trust region reflective techniques (Sharifzadeh et al., 2018b; Senatore et al., 2017; Sharifzadeh et al., 2018a).

$$\begin{cases} \epsilon(k, \theta) = y(k) - \hat{y}(k|\theta) \\ \hat{x}(k+1) = \theta_A \hat{x}(k) + (\theta_B + \theta_F) u(k) \\ \hat{y}(k|\theta) = \theta_C \hat{x}(k) + (\theta_D + \theta_E) u(k) \end{cases} \quad (4)$$

Given the relatively small scale of the HVAC model, with limited inputs, outputs, and state variables, the use of the presented method does not lead to

significant computational challenges. Moreover, the iterative nature of PEM aligns well with the requirements of real-time implementation, ensuring efficient integration into the control loop.

5 CONTROL DESIGN

5.1 Design of Specific Controllers

Considering the given discrete linear time-invariant system to be controlled above: $x(t+1) = Ax(t) + Bu(t) + Fw(t)$ and $y(t) = Cx(t)$, where $A \in \mathbb{R}^{n \times n}$ is the state matrix, $B \in \mathbb{R}^{n \times p}$ is the control input matrix, $F \in \mathbb{R}^{n \times p}$ is the measured disturbance matrix, $x(t) \in \mathbb{R}^n$ is the state variable, $u(t) \in \mathbb{R}^p$ is the control input variable, $y(t) \in \mathbb{R}^q$ is the output variable, and $C \in \mathbb{R}^{q \times n}$ is the output matrix. where MPC determines the optimal strategy for the current state by applying the optimization problem for $x(k)$, aiming to minimize the cost function outlined below:

$$\begin{aligned}
J^*(x(t)) = & \min_{U \triangleq [u_1^T \dots u_{t+M-1}^T]^T} \\
& F_N(x(t+N)) + \sum_{k=0}^{N-1} F_k(x(t+k|t), u(t+k)) \\
\text{subject to} & \\
& u_{\min} \leq u(t+k) \leq u_{\max}, \quad k = 1, \dots, M-1 \\
& \delta u_{\min} \leq \delta u(t+k) \leq \delta u_{\max}, \quad k = 1, \dots, M-1 \\
& y_{\min} \leq y(t+k|t) \leq y_{\max}, \quad k = 1, \dots, N \\
& x(t+k+1|t) = Ax(t+k|t) + Bu(t+k) + Fw(t+k), \\
& y(t+k) = Cx(t+k|t), \quad k \geq 0
\end{aligned} \tag{5}$$

where

$$\begin{aligned}
F_N(x(t+N)) &= \|x(t+N) - r(t)\|_{\mathbb{P}}^2 \\
F_k(x(t+k|t), u(t+k)) &= \|x(t+k) - r(t)\|_{\mathbb{Q}}^2 \\
&+ \|u(t+k) - u_r(t)\|_{\mathbb{R}}^2
\end{aligned}$$

having $Q = Q^T \geq 0$, $R = R^T > 0$, $P \geq 0$, $x(t+k|t)$ is the prediction of $x(t+k)$ at time t hence, $x(t|t) = x(t)$ and N and M are prediction and control horizons. When the matrices P and K could be obtained the algebraic Riccati equation, which eventually solves the constrained problem above, having the weight matrices R and Q .

As given above for the saving energy by optimization of constraints it is possible to set the desired constraints in $u_{\min} \leq u(t+k) \leq u_{\max}$ and $\delta u_{\min} \leq \delta u(t+k) \leq \delta u_{\max}$.

Regarding the Defrost modality, since the objective is to achieve pre-specified compressor frequency targets, a PID controller is selected for this mode. Advanced control strategies are considered unnecessary for this modality due to its simple control requirements.

5.2 Switching Logic Design

As illustrated in Fig. 3, the model considers four states Initial_Off, HeatCool, Off and Defrost. From which HeatCool and Off are serving as hierarchical states.

Table 1: High-level logical specifications at Fig. 3.

Guard	Definition
Cond_Off	$\text{TrmOff} \vee \text{UsrOff} \vee \text{AL_Off} \vee \text{AL_StComp}$
Cond_HeatCool	$(\text{HPL_PINotPr} \vee \text{HPL_PIPr} \vee \text{HDHW1} \vee \text{HDHW2} \vee \text{CL_PINotPr} \vee \text{CL_PIPr}) \wedge (\text{Alarm_must_off} = \text{AL_Off_N} \wedge \text{Alarm_force_stop_comp} = \text{AL_St_Comp_N}) \wedge (\text{Defrost_need} = \text{Def_N} \vee \text{Defrost_need} = \text{Def_to_be_Act})$
Cond_Defrost	$\text{Alarm_must_off} = \text{AL_Off_N} \wedge \text{Alarm_force_stop_comp} = \text{AL_St_Comp_N} \wedge \text{Defrost_need} = \text{Def_Act}$

The transitions between the primary states are constrained by three specific guards: Cond_Off, Cond_HeatCool, and Cond_Defrost, whose definitions are provided in Table 1. The hierarchical state HeatCool decomposes into the sub-states Heating_DHW, Heating_Plant, and Cooling_Plant, with their own model and further transitions between these substates governed by specific guards and accompanied by effects associated with each state. The hierarchical state Off is divided into three sub-states Off by Alarm, Off by Thermal, and Off by User as well. The effect in these three sub-states is a control action that turns off the compressor.

In the Off by Alarm sub-state, the compressor is turned off immediately, whereas in the Off by User and Thermal Off sub-states, it turns off within a specific period unique to each sub-state.

Table 2: Identifiers used in the logic and their descriptions.

Identifier	Definition	Value	Description
Defrost_need	Checking the need for defrosting	Def_Act	Defrost is activated
		Def_N	Defrost is not active
		Def_tobe_Act	Defrost to be activated
Alarm_force_stop_comp	Checking if the compressor is forced to stop due to an alarm	AL_St_Comp_N	Compressor is not forced to stop due to an alarm
		AL_St_Comp_Act	Compressor is forced to stop due to an alarm
Alarm_must_off	Checking if it must be off due to an alarm	AL_Off_Act	It must be off due to an alarm
		AL_Off_N	It must not be off due to an alarm

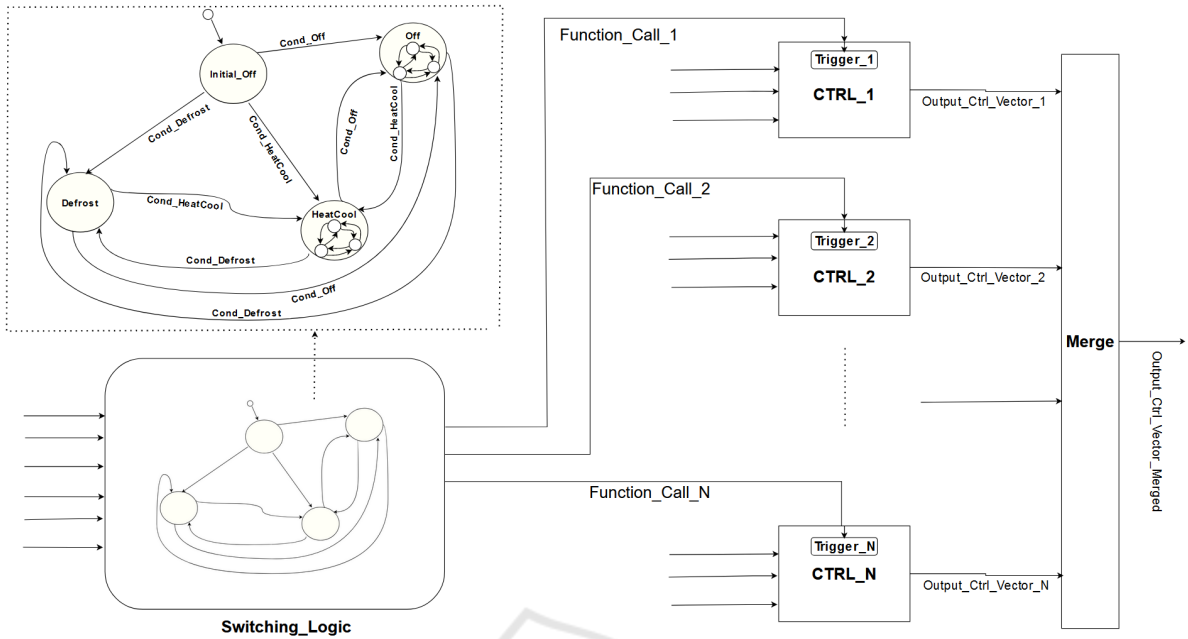


Figure 3: The Scheme of the Switching Event-Triggered MPC.

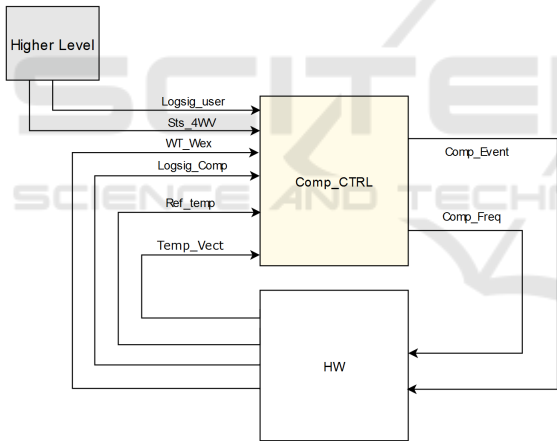


Figure 4: Component Control Scheme.

MPC is designed for each of these three sub-states. The conditions HPL_PIPr and HPL_PINotPr represent the heating plant mode, indicating whether the plant is prioritized or not, respectively. Similarly, CL_PIPr and CL_PINotPr denote the cooling plant whether the plant is prioritized or not. Two separate conditions, HDHW1 and HDHW2, specify when Heating_DHW should be activated. Additionally, TrmOff and UsrOff, which are two of four specified conditions for the state Off (see Table 2), define the conditions under which the system should be deactivated due to thermal reasons and user intervention, respectively. As also shown in Fig. 3, each function call triggers an event for each modality/functionality.

6 RESULTS

In this section, the previously presented approach will be illustrated and applied to the use case described earlier. A test is conducted to check the identified model and validate the control approach using switching scenarios. All computations are carried out on an Intel Core i7-8650U with 4 cores, at 1.90 GHz, with 32 GB RAM, running Matlab R2019b and Python 3.9.13. The Model Predictive Control 6.3.1 and Embedded Coder 7.3 Toolboxes are utilized for the MPC object and code generation respectively. The refined version of this generated code gives a standalone code that is designed in a way that makes it easily expandable for future updates and integration.

6.1 Validation of the Identified Model

As for the system identification, using the refined time series data and dividing it into two sets of training and validation data, within different periods of the year for the different modalities, with a sampling frequency of 20 Hz for both datasets and applying the constraints (e.g., $CompFreq < 120 \text{ Hz}$) is considered for the validation. The cross-validation results presented in Table 3 illustrate the Mean Absolute Error (MAE) values for different months of the heating plant, indicating the accuracy of the identified system output compared to the real acquired data points. The table covers the period from November 2022 to

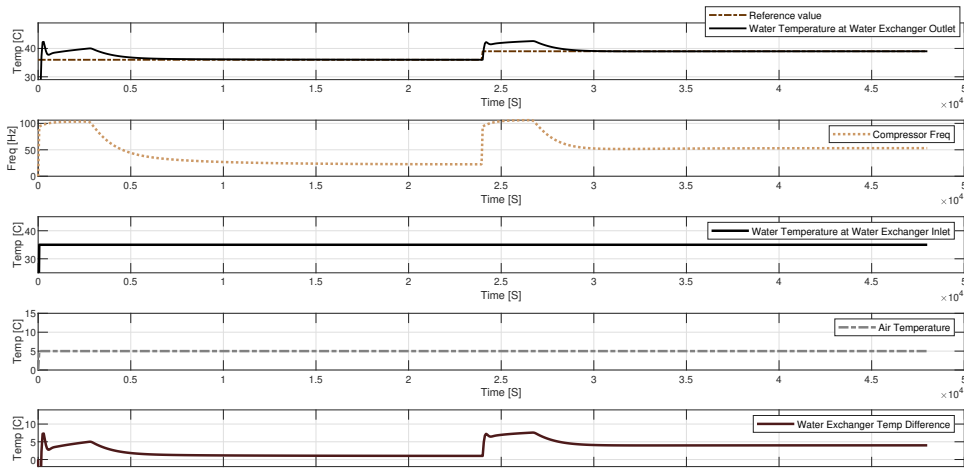


Figure 5: Time history of the measured temperature for the components and the Compressor Frequency.

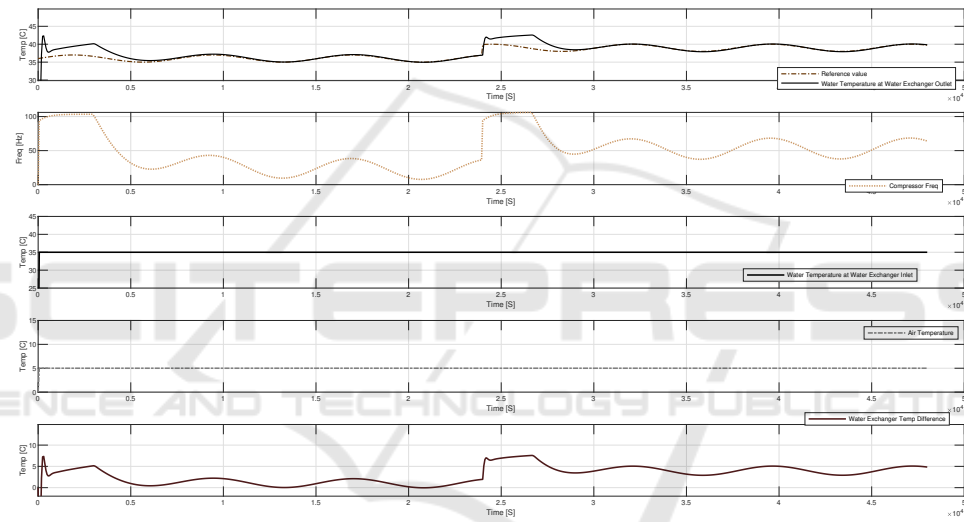


Figure 6: Time history of the measured temperature for the components and the Compressor Frequency having disturbance.

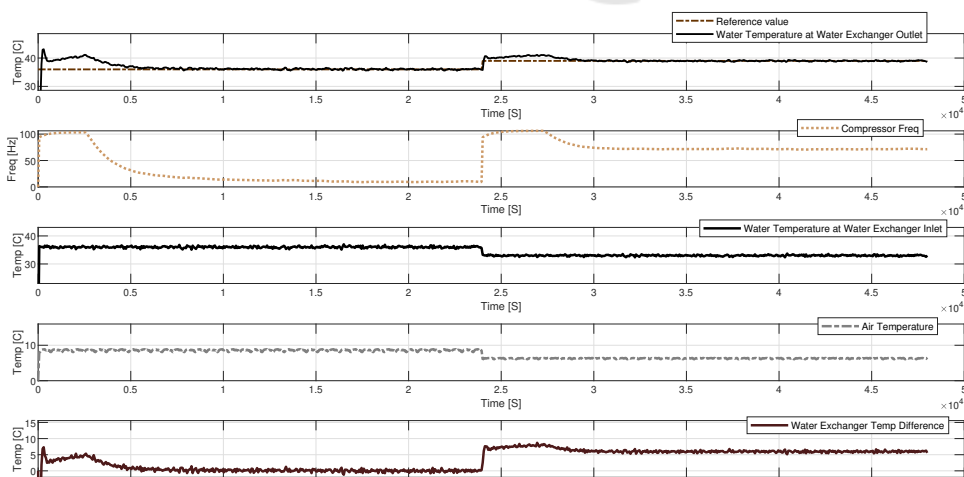


Figure 7: Time history of the measured temperature for the components and the Compressor Frequency during uncertainty.

March 2023. Each row represents the MAE for the output difference explained earlier when trained for one month and validated against the others. The diagonal elements are zero, reflecting the comparison of the model output against the same month. These results underscore the model's robustness and areas for improvement in predicting specific monthly outputs. Moreover, it also considered to check observability and the controllability of the obtained models. The obtained systems are both controllable and observable as $\text{rank}[B, AB, A^2B] = 4$ and $\text{rank}[C, CA, CA^2] = 4$.

Table 3: Cross-validation results.

	Nov 22	Dec 22	Jan 23	Feb 23	Mar 23
Nov 22	0	1.1408	1.0915	1.0636	1.0652
Dec 22	0.6863	0	1.0729	1.0240	0.9041
Jan 23	0.6668	1.1387	0	0.9789	0.8843
Feb 23	0.6587	1.1160	1.0356	0	0.9606
Mar 23	0.8867	1.3945	1.2833	1.2106	0

Table 4 presents given MAE values for three different operational modes—Heating Plant, Heating DHW, and Cooling—using varying numbers of state variables (3, 4, and 5). According to the MAE results for all three modalities, the obtained model exhibits accurate performance. Additionally, the MAE remains relatively stable across different numbers of state variables.

Table 4: MAE for various modalities with different numbers of state variables.

Modality	State Variables	MAE
Heating Plant	3	1.0132
	4	1.0122
	5	1.0674
Heating DHW	3	0.9786
	4	0.9777
	5	0.9785
Cooling	3	0.8499
	4	0.8492
	5	0.8323

6.2 Performance Analysis of the Proposed Control Approach

In order to evaluate the performance of the given control strategy, MIL testing is carried out in various scenarios. Fig. 5 is the first test showing the time history of the measured values in the HVAC system,

which switches from the Heating DHW modality to the Heating Plant at time 2.4×10^4 . The first plot illustrates a precise reference trajectory tracking, where the water temperature at the Water Exchanger Outlet follows the reference value. The second sub-figure shows that the Compressor Frequency performs as expected over time, especially during the switching period. The third sub-figure shows the water temperature at the Water Exchanger Inlet. The time history of the air temperature and the water temperature difference at the Water Exchanger are shown in the last two sub-figures, respectively. N and M at MPC are set as 600 s and 120 s where $Q = 1$ and $R = .1$.

In the second scenario in Fig. 6, the performance is tested with a harmonic disturbance. As shown, it provides an acceptable settling time during the test. In the third scenario at Fig. 7, Gaussian random noise is introduced for both the water temperature at the Water Exchanger Outlet and the air temperature. The test is performed under different conditions involving a rapid fluctuation in the temperature at the Water Exchanger Outlet. It demonstrates an acceptable tracking of the reference trajectory, with the overshoot remaining within an acceptable range. The control approach exhibits robust performance in the presence of harmonic disturbances which demonstrates robust performance against Gaussian noise. Furthermore, it is possible to achieve additional reductions in the Integrated Absolute Error (IAE) by optimizing the MPC (Model Predictive Control) parameters.

7 CONCLUSION

In this paper, we presented a new switching control methodology based on function calls that trigger events for each functionality/modality, enhancing the efficiency and functionality of the HVAC application. A new model for model-based control was developed and validated using acquired data from machines in the test field. This model was also implemented in the MPC framework and tested through MIL testing in various machine modalities. As future work, we intend to deploy and validate the code generated from the proposed model on the field. We currently have provided the artefacts in a file available at <https://es-static.fbk.eu/people/ssharifzadeh/ICINCO2024/>.

ACKNOWLEDGEMENTS

The work is financed by the Autonomous Province of Trento in the scope of L.P. No. 6/1999 with determination. No. 592 of 09/08/2021. – Ref.: 2021-AG12-

00783. - project NPDCR (Nuova Pompa di Calore Residenziale - New residential heat pump).

Yao, Y. and Shekhar, D. K. (2021b). State of the art review on model predictive control (mpc) in heating ventilation and air-conditioning (hvac) field. *Building and Environment*, 200:107952.

REFERENCES

- Afroz, Z., Shafiullah, G., Urmee, T., and Higgins, G. (2018). Modeling techniques used in building hvac control systems: A review. *Renewable and sustainable energy reviews*, 83:64–84.
- Blasco, C., Monreal, J., Benítez, I., and Lluna, A. (2012). Modelling and pid control of hvac system according to energy efficiency and comfort criteria. In *Sustainability in Energy and Buildings: Proceedings of the 3rd International Conference in Sustainability in Energy and Buildings (SEB'11)*, pages 365–374. Springer.
- Darby, M. L. and Nikolaou, M. (2012). Mpc: Current practice and challenges. *Control Engineering Practice*, 20(4):328–342.
- Ljung, L. (1998). System identification. In *Signal analysis and prediction*, pages 163–173. Springer.
- Saletti, C., Gambarotta, A., and Morini, M. (2020). Development, analysis and application of a predictive controller to a small-scale district heating system. *Applied Thermal Engineering*, 165:114558.
- Senatore, A., Pisaturo, M., Sharifzadeh, M., et al. (2017). Real time identification of automotive dry clutch frictional characteristics using trust region methods. In *AIMETA 2017-Proceedings of the XXIII Conference of the Italian Association of Theoretical and Applied Mechanics*, pages 526–534. AIMETA-Associazione Italiana di Meccanica Teorica e Applicata.
- Sharifzadeh, M., Pisaturo, M., Farnam, A., and Senatore, A. (2018a). Joint structure for the real-time estimation and control of automotive dry clutch engagement. *IFAC-PapersOnLine*, 51(15):1062–1067.
- Sharifzadeh, M., Senatore, A., Farnam, A., Akbari, A., and Timpone, F. (2018b). A real-time approach to robust identification of tyre-road friction characteristics on mixed- μ roads. *Vehicle system dynamics*.
- Soyguder, S., Karakose, M., and Alli, H. (2009). Design and simulation of self-tuning pid-type fuzzy adaptive control for an expert hvac system. *Expert systems with applications*, 36(3):4566–4573.
- Staino, A., Nagpal, H., and Basu, B. (2016). Cooperative optimization of building energy systems in an economic model predictive control framework. *Energy and Buildings*, 128:713–722.
- Taheri, S., Amiri, A. J., and Razban, A. (2024a). Real-world implementation of a cloud-based mpc for hvac control in educational buildings. *Energy Conversion and Management*, 305:118270.
- Taheri, S., Amiri, A. J., and Razban, A. (2024b). Real-world implementation of a cloud-based mpc for hvac control in educational buildings. *Energy Conversion and Management*, 305:118270.
- Yao, Y. and Shekhar, D. K. (2021a). State of the art review on model predictive control (mpc) in heating ventilation and air-conditioning (hvac) field. *Building and Environment*, 200:107952.